REPORT DOCUMENTATION PAGE

Form Approved
OMB No. 0704-0188

1. AGENCY USE ONLY *(Leave blank)*	2. REPORT DATE	3. REPORT TYPE AND DATES COVERED
	April 1996	Journal Article, March 1989–March 1992

4. TITLE AND SUBTITLE
Grating Visual Acuity Following Hemorrhagic Foveal Lesions

5. FUNDING NUMBERS
C - F33615-88-C-0631
PE - 62202F
PR - 7757
TA - 02
WU - 96

6. AUTHOR(S)
James W. Rhodes and Paul V. Garcia

7. PERFORMING ORGANIZATION NAME(S) AND ADDRESS(ES)
KRUG Life Sciences Inc.
San Antonio Division
P.O. Box 790644
San Antonio, TX 78279-0644

8. PERFORMING ORGANIZATION REPORT NUMBER

9. SPONSORING/MONITORING AGENCY NAME(S) AND ADDRESS(ES)
Armstrong Laboratory
Occupational and Environmental Health Directorate
Optical Radiation Division
8111 18th Street
Brooks Air Force Base Texas 78235-5215

10. SPONSORING/MONITORING AGENCY REPORT NUMBER
AL-JA-1992-0063

11. SUPPLEMENTARY NOTES
Lasers and Light in Ophthalmology, 7(4), 1996, pp. 153-165.

12a. DISTRIBUTION/AVAILABILITY STATEMENT
Approved for public release; distribution is unlimited.

12b. DISTRIBUTION CODE

13. ABSTRACT *(Maximum 200 words)*
Grating visual acuity was measured in three cases of experimentally produced foveal, hemorrhagic vitreous lesions in rhesus monkeys. A dual-Purkinje-image (DPI) eye-tracker and a modified laser photocoagulator were used to target the laser exposure while the subject was engaged in an operantly trained grating detection task. Each subject received one exposure in the right eye from a Q-switched Nd:glass laser. The resulting vitreous hemorrhage emanated from a disk-shaped area of edema and disrupted tissue; the blood was largely confined to a single, inferiorly directed column, with only slight, diffuse mixing with the vitreous. Grating acuity in the injured eye declined immediately after the laser exposure. During the ensuing 37-day assessment period, acuity returned to the pre-exposure range within 5 to 14 days. The size of the area of retinal injury also decreased over the assessment period, but complications of vitreous clouding and strial traction lines were noted.

14. SUBJECT TERMS
Lasers; Retinal hemorrhage; Retinal laser injury; Visual acuity

15. NUMBER OF PAGES
13

16. PRICE CODE

17. SECURITY CLASSIFICATION OF REPORT	18. SECURITY CLASSIFICATION OF THIS PAGE	19. SECURITY CLASSIFICATION OF ABSTRACT	20. LIMITATION OF ABSTRACT
Unclassified	Unclassified	Unclassified	UL

Lasers and Light vol. 7 no. 4 pp 153-165 (19
Kugler Publications, Amsterdam/New Y

Grating visual acuity following hemorrhagic foveal lesions

James W. Rhodes and Paul V. Garcia
KRUG Life Sciences, Inc., San Antonio, TX, USA

Keywords: lasers, visual acuity, retinal laser injury, retinal hemorrhage

Abstract

Grating visual acuity was measured in three cases of experimentally produced foveal, hemorrhagic vitreous lesions in rhesus monkeys. A dual-Purkinje-image (DPI) eyetracker and a modified laser photocoagulator were used to target the laser exposure while the subject was engaged in an operantly trained grating detection task. Each subject received one exposure to the right eye from a Q-switched Nd:glass laser. The resulting vitreous hemorrhage emanated from a disc-shaped area of edema and disrupted tissue; the blood was largely confined to a single, inferiorly directed column. Grating acuity in the injured eye declined immediately after the laser exposure. During the ensuing 37-day assessment period, acuity returned to the pre-exposure range within five to 14 days. The size of the area of apparent retinal injury and obscuration also decreased over the assessment period, but complications of vitreous clouding and traction lines were noted.

Introduction

Ocular laser exposures sufficiently intense to cause vitreous hemorrhage can be achieved by many of the lasers currently employed in laboratory, industrial, and military settings. The typical source of hemorrhage is rupture of choroidal vessels. Released blood can pool beneath the retinal pigment epithelium (RPE) and/or the retina. In the case of vitreous hemorrhage, blood also escapes into the vitreous cavity through a channel formed by local destruction of the retina, the RPE, and Bruch's membrane. Blood that mixes with the vitreous or that spreads along the vitreous-retinal interface can affect non-damaged portions of the retina by producing a veiling haze or blocking defect.

Case studies of accidental layer eye injury have documented the deleterious consequences of retinal hemorrhage. The effect of the hemorrhage-producing laser exposure is typically immediate and severe. Accident victims sometimes experience complete loss of vision in the affected eye, although that condition is transitory[1]. Other, more typical symptoms include scotomas, blur, or haze in the visual field. Visual capacity, as assessed by standard clinical tools, such as the Snellen acuity eye chart, invariably shows a deficit if the injury directly or indirectly involves the fovea, and especially, the foveola. The extent to which acuity and related measures of spatial resolution ability are depressed appears to be quite variable across cases, although a minimum angle of resolution (MAR) of 5 arcmin or higher is not uncommon[1]. Little, if any, measurable loss of acuity is seen if the injury site is extrafoveal and if no blood obscures the foveal area. An exception to this generalization can occur if the papillo-macular bundle is significantly disturbed by the injury[2].

Partial recovery of visual acuity takes place in almost all hemorrhage-producing retinal injuries, and in some cases, the degree of recovery is dramatic[3]. As with the acute effects of the injury, the prognosis is variable. Complicating factors include the formation of scar tissue, retinal detachment, and striae radiating outward from the border

Address for correspondence: James W. Rhodes, PhD, Department of Biosciences and Bioengineering, Southwest Research Institute, P.O. Drawer 28510, San Antonio, TX 78228-0510, USA
The research reported here was supported by Contract F33615-88-C-0631, let by the Armstrong Laboratory, Brooks AFB, TX, USA

of the wound. These side effects of tissue healing have been implicated in some cases where acuity initially improved after the injury, and then declined[4].

Only a small number of studies have experimentally investigated foveally centered vitreous hemorrhages in higher, non-human primates as a model for laser accident cases. Glickman *et al.*[2] measured grating acuity electrophysiologically in the anesthetized rhesus monkey using the spatial frequency swept VEP technique. Baseline, pre-exposure MARs were 2.00 to 2.25 arcmin. Immediately after laser-produced vitreous hemorrhage, a brief period ensued in which no VEPs could be elicited. When VEPs could again be measured, MARs averaged 3.00 to 4.00 arcmin, but could transiently increase to more than 10 arcmin over the first post-exposure hour. One of the two subjects recovered to pre-exposure baseline (2.25 arcmin); the other subject stabilized at 3.00 arcmin. Graham *et al.*[5] measured operant discrimination for two-alternative forced choice detection by rhesus monkeys of a 5-arcmin gap in a Landolt ring before and immediately after monocular laser exposure. Performance in the exposed eye fell to chance level in all four subjects sustaining a vitreous hemorrhage; performance in the non-exposed eye was at or near pre-exposure baseline in three of the four subjects. Other, similar studies of ocular laser exposure on visual acuity have not employed vitreous hemorrhage as a damage endpoint[6].

We sought to extend the limited database on the acute and chronic effects of hemorrhagic retinal lesions using the rhesus monkey as a subject. This species has been frequently selected as a model for light-induced retinal damage because of the strong similarity of its visual system to that of the human[7,8]. Such functions as acuity[9-12], spatial and temporal contrast sensitivity[13], and spectral sensitivity[14,15], have been measured in the light-damaged retina of the rhesus monkey. In the present study, a behavioral psychophysical method was developed to acquire grating acuity at a rapid temporal sampling rate, so that the immediate as well as the longer-term retinal lesion effects could be measured.

Methods

Subjects

Three rhesus monkeys (*Macaca mulatta*) were used as subjects. One was a young female (Subject 2), two years old and weighing 4.5 kg. The others (Subjects 1 and 3) were male, five years of age, and weighed approximately 9 kg each. All subjects were given ophthalmic examinations under Nembutal (20 mg/kg) anesthesia, with mydriasis produced by topical 1% atropine sulfate (Alcon). Refractive error was evaluated by streak retinoscopy using hand-held trial lenses, and the ocular fundus was documented by white light photography and fluorescein angiography.

Research animals involved in this study were procured, maintained, and used in accordance with the Animal Welfare Act and the 'Guide for the Care and Use of Laboratory Animals' prepared by the Institute of Laboratory Animal Resources – National Research Council.

Eye tracking and fundus visualization

Eye position was monitored by a DPI eyetracker (Generation V, Fourward Technologies, Inc.). Infrared illumination was used to produce Purkinje reflections from the cornea and lens of the subject's eye, which were captured by the eyetracker optics to measure rotational and translational eye position[16]. The Fundus Illumination and Measurement Instrument (FIMI) (Fourward Technologies, Inc.) allowed the experimenter to visualize the fundus and to focus and stabilize the optical path of a laser beam at a selected location on the fundus. To aid fundus visualization with the FIMI, one drop of atropine sulfate (1%) was instilled as needed onto the cornea of the right eye to produce long-lasting mydriasis.

Optical system

Figure 1 schematically illustrates the optical system, consisting of: *1.* the DPI eyetracker; *2.* FIMI and video camera; *3.* an optical channel for presentation of the visual detection stimuli; and *4.* a channel for the laser.

Left and right eye views of the visual detection stimuli were controlled by a shutter (SH) and a

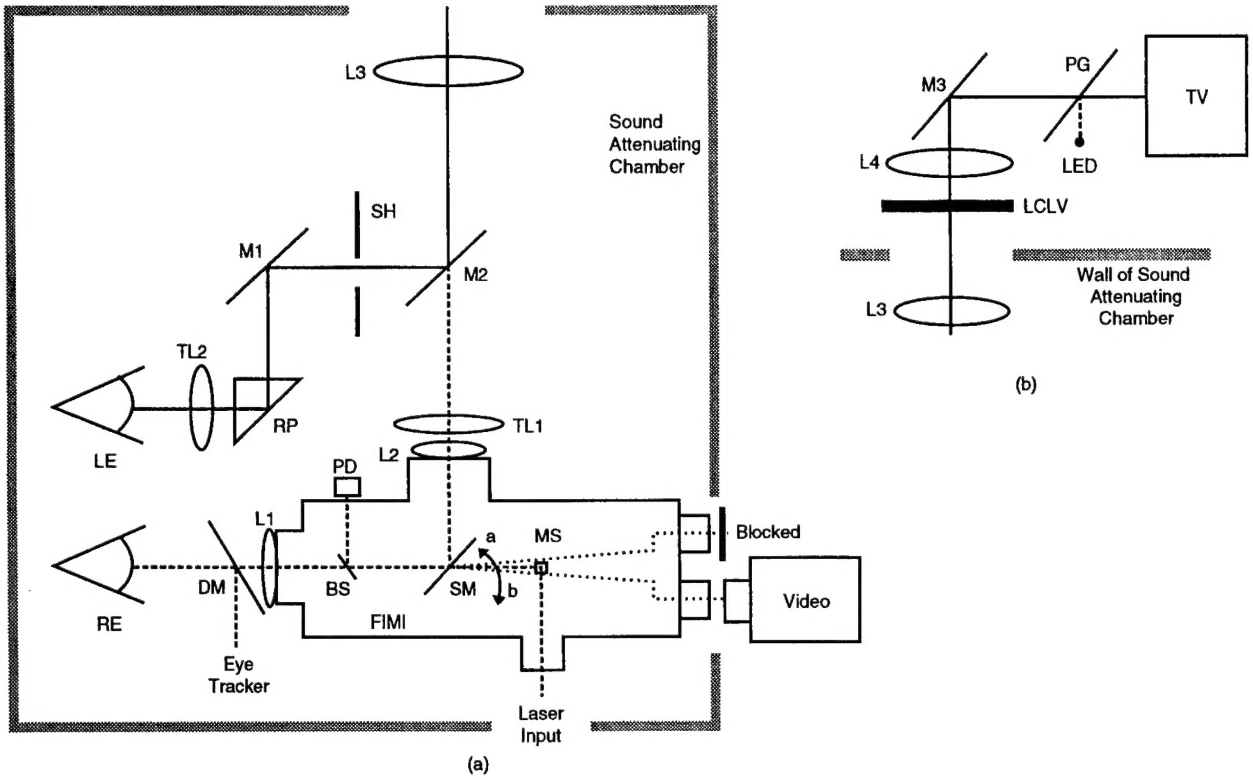

Fig. 1. Visual stimulus optical system. In Part a of the figure, the optics proximal to the subject's eye are shown. The left eye (LE) viewed the visual stimulus through beamsplitter M2 and an optical path consisting of shutter SH, mirror M1, right-angle prism RP, and trial lens TL2 to correct for refractive error. The right-eye (RE) optical pathway joined the LE pathway at beamsplitter M2 via lens L1, swing-out mirror SM, and lenses L2 and TL1. A dichroic mirror (DM) transmitted visible light, but reflected narrow bandwidth, near-infrared light used by the DPI eyetracker. Part b shows the remainder of the visual stimulus channel located outside the sound attenuating chamber. The stimulus field was produced by a television monitor (TV) and was directed to the subject through beamsplitter PG, mirror M3, lens relay pair L3-L4, and liquid crystal light valve LCLV, which functioned as a shutter. An LED was positioned above a plate-glass beamsplitter (PG) and projected a virtual image coplanar with the TV screen.

solenoid-driven, swing-out mirror (SM), respectively. These two devices were slaved together so that when the shutter was closed, the swing-out mirror was in Position a (Fig. 1), allowing the right eye to view the visual stimulus channel. Conversely, when the shutter was opened, permitting the left eye to view the visual stimulus channel, the swing-out mirror was in Position b, which eliminated right eye access to the visual channel. Thus, the subject's viewing condition was always dichoptic. With the swing-out mirror in Position b, the laser beam optical path was also unblocked and the fundus could be visualized by the video camera.

The laser beam input into the right eye was directed and stabilized by the FIMI, using eyetracker inputs. Since the optics and control principles of the FIMI have been described in detail elsewhere[16,17], only the key points will be summarized here. The laser entered the FIMI through an input port and was directed by stationary mirrors onto a pair of galvanometer-mounted mirrors (not shown), optically conjugate to the center of rotation of the subject's eye. When the eyetracker was properly calibrated, the movable mirrors turned in synchrony with the eye, thereby stabilizing the laser beam at a point on the retina. By controlling the offsets of the galvanometers, the position of the laser on the retina could be selected. This was aided by illuminating the fundus through the FIMI optics and observing it with a color video camera (Panasonic, Digital 5000).

Visual stimuli

The visual stimulus field was a disc-shaped area 9.3 degrees in diameter at a viewing distance of 158.5 cm. Unless a grating pattern was being displayed, the field was homogeneous and achromatic, except for the superimposed image of a single, illuminated, red light-emitting diode (LED) that served as a fixation target.

Square-wave luminance gratings were displayed on a high resolution black and white television monitor (Video Monitors, Inc., 2400 Series) having a 1024-by-1024 raster and a frame rate of 71 Hz. The percent contrast of the gratings was computed as [(Lmax – Lmin)/(Lmax + Lmin)] * 100, where Lmax and Lmin were the luminance in candelas per square meter (cd/m^2) of the light and dark bars. Measured contrast was between 81% and 87% for the highest and lowest spatial frequencies, respectively.

The spatial frequency of the gratings was varied from 0.4 to 26.0 cycles per degree (cpd) in unequal steps. Higher spatial frequencies were not possible with the field size and viewing distance used. The spatial frequencies and their MAR equivalents are shown in Table 1. MAR was based on the angular subtense of a grating half-cycle (*e.g.*, 30 cpd was equivalent to a 1.0 arcmin MAR).

Photometric measurements of the television raster were made with a Pritchard 1980A spectrophotometer. To derive a linear scale of television monitor luminance, a 15-point gamma correction was made using the photometer's 6-arcmin measuring field. Luminance of the homogeneous stimulus field was 30.3 cd/min^2. This was confirmed by measurement. As a result, there was no brightness change associated with either onset or termination of grating presentation that could serve as a detection cue.

Three-axis positioning system

The DPI eyetraker required that the subject's eye stay within a small volume of space. Positioning of the subject's eye was accomplished by the combination of a restraint chair, a face mask anchored to the restraint chair, and a motorized platform on which the restraint chair was placed. The subject maintained a comfortable, species-typical crouching posture in the restraint chair and could easily reach the response lever attached onto the front of the chair. The face mask, which was made of molded dental acrylic and containing openings for the eyes and snout, was necessary for stabilization of the subject's head position. After the subject was secured in the restraint chair, it was placed on a three-dimensional, motorized platform located inside a sound-attenuated testing chamber. Remote operation of the motorized platform allowed the experimenter to position the subject's eye within the 'capture' range of the eyetracker, even while the subject performed the grating detection task. Rhesus subjects stayed in the restraint chair only for the duration of a daily training and testing session of about one hour.

Table 1. Equivalent angular dimensions of square-wave grating stimuli

Spatial frequency (cpd)	*Minimum angle of resolution (arcmin)*
0.4	75.0
0.8	37.5
1.6	18.8
2.4	12.5
3.2	9.4
4.7	6.4
6.5	4.6
8.7	3.4
10.4	2.9
13.0	2.3
17.3	1.7
26.0	1.2

Laser

Retinal lesions were produced by a single pulse from a neodymium:glass (Nd:glass), Q-switched laser (Laser Applications, Inc., Model 933G3L-3). The output of the Nd:glass laser had a wavelength of 1060 nm and a pulse width of 20 nsec. Laser exposure energy at the subject's cornea was measured by a radiometer (Photodyne Model 66XLA) equipped with an integrating sphere that directed the laser output onto a photodiode calibrated at 1060 nm (Photodyne Detector, Model 350). The laser beam was collected by a 95%T5%R beamsplitter (BS) located between mirror MS and lens L1 (see Fig. 1). Energy readings from the radiometer (PD, Fig. 1) adjacent to the BS were cross-

calibrated with another radiometer of the same make and model placed at the subject's eye position.

A helium-neon (HeNe) laser, colinear with the Nd:glass laser, was used for alignment. Both laser beams were substantially smaller than the entrance pupil of the subject's eye. Power at the cornea from the HeNe laser was measured to be 0.1 mW, a level well within the safety standards developed by the American National Standards Institute[18].

Behavioral task

The subject was trained to press a response lever when a visual stimulus was presented. The stimulus could be a momentary decrement in the steady-state brightness of an LED fixation target, or it could be the presentation of a square-wave luminance grating. Either of the two stimulus events lasted 0.5 sec. The subject had 0.9 sec, starting with stimulus onset, to press the response lever. A correct response occurred if, and only if, a lever response fell within the 0.9-sec temporal window. Correct responses were reinforced with a small amount of orange drink on a 50% probability basis. Data collection, behavioral task contingencies and peripheral device control were implemented through a laboratory microcomputer (Zenith, Model 2WX-0248-62) and custom software written in Turo Pascal, ver. 5.5.

To optimize the reinforcement value of the orange drink, the subjects were placed on a water-restriction schedule lasting no more than five days out of a seven-day week. During water restriction, the subject's only source of liquid was through performance in the behavioral task. Water was available *ad libitum* during weekends, and when the water restriction schedule was not in effect. All subjects gained weight over the course of the study and were judged to be healthy on the basis of periodic examinations made by staff veterinarians.

The stimulus level was controlled by a psychophysical titration schedule[19,20]. In the case of the LED fixation target, a correct response resulted in a smaller brightness decrement on the next occurrence of the LED stimulus. Likewise, an incorrect response increased the brightness decrement magnitude. Successive correct responses lowered the amount of brightness change until the subject's detection threshold was reached or the lowest programmed brightness decrement was encountered. An identical, but independent schedule controlled the spatial frequency of the square-wave luminance grating. A correct response increased grating spatial frequency by one step, whereas an incorrect response produced a step-wise decrease in spatial frequency.

Pre-exposure performance baselines

Detection performance baselines were acquired on both the LED fixation target and the square-wave luminance grating. The criterion for acceptable LED performance was that the subject maintain the brightness decrement in the lowest one-third of the brightness change continuum. Performance at this level served to keep the subject's right eye within the capture and laser beam optical path stabilization limits of the eyetracker/FIMI. The minimum baseline performance standard for grating acuity was 14 cpd (2.3 arcmin) on at least 85% of the trials. All subjects produced at least 15 acceptable baselines prior to laser exposure.

Identification of the foveola

The target for laser exposure was the foveola. In humans, the foveola is sometimes distinguished by a light reflex[21]. Unfortunately, the foveolar reflex was not discernible in the video fundus image of the rhesus monkey subjects, but the pigmentation in the vicinity of the foveola was typically darker than that of the rest of the macula. Therefore, an area in the approximate center of the macula was used that corresponded to a region of relatively dark pigmentation as the marker for identification of the foveola. Color fundus photographs of each subject were shown to optometrists and ophthalmologists who had experience in ophthalmic examinations of rhesus monkeys, and in every case, their judged location of the foveola corresponded with the location used. These fundus photographs were used as references in selecting the foveolar target for laser exposure.

Lesion size produced by laser exposure was estimated from fundus photographs. The lesion was identified as the area obscuring the normally visible funduscopic details. Size was measured in

terms of the horizontal diameter of the optic disc also visible in the fundus photographs.

Requirements for laser exposure

The experiment control software continually sampled ten control variables and compared their boolean states by a logical 'and' operation. A logical 'true' was necessary for a laser exposure and indicated that the subject's acuity performance was within criterion, that the eye to be laser-exposed was being accurately tracked, and that the intratrial, predetermined temporal window for a laser exposure was in effect.

Definition and analysis of grating visual acuity

Acuity was defined as the spatial frequency occurring midway between the spatial frequencies associated with a pair of contiguous responses in which one was correct and the other was incorrect. Acuity means and standard deviations were computed for the left and right eye of each subject over the course of pre-exposure baseline acquisition and post-exposure evaluation. A one-way analysis of variance was performed on the pre-exposure data to derive estimates of within- and between-session variance components. These estimates were used to compute upper and lower 95% confidence limits (C.I.) against which post-exposure session acuities could be compared. Each individual was considered as a 'case study', in that data across subjects were not pooled, and separate confidence limits were established for each subject.

The left eye of each subject was not laser-exposed. Grating acuity measured in the left eye was used as an indicator of the on-task performance status of the animal throughout the pre- and post-laser exposure measurement periods. A drop in the acuity of the right, laser-exposed, eye could reflect either a general impairment of motivation to perform the behavioral task, or diminished spatial resolution capability in the damaged eye, or both. If left eye acuity remained within the baseline range, then any reduction in right eye acuity within a measurement session could be more directly attributed to visual degradation.

Because of the brief viewing time for a grating presentation (0.5 sec) and the high spatial frequency limitation (26 cpd), pre-laser exposure acuities were less than that measured for rhesus monkeys under conditions that optimize spatial resolution. Since the main concern was capture of the relatively low grating acuity levels expected to follow placement of hemorrhagic foveal lesions, measurement of the highest possible spatial resolution was not considered necessary.

Results

All subjects sustained a vitreous hemorrhage from a laser exposure of 0.5 to 7.2 mJ total intraocular energy (TIE), on or near the foveola. Summary statistics and the principal effects associated with the laser exposures are summarized in Table 2.

Initial laser exposure effects

Laser exposure was followed by an immediate, but temporary interruption or cessation of behavioral task performance of 1.0 to 4.6 minutes in duration. Upon recovery of task performance, acuity measurement proceeded for three to 24 minutes, resulting in 14 to 138 individual acuity estimates. Longer measurement periods were not possible because most of the one-hour session was taken up with baselining and preparations for laser exposure.

Measured acuity hovered about a new, lower, average value that in all cases was below the lower 95% C.I. Individual acuity estimates sporadically dropped to even lower levels; this was especially marked in Subject 3 which received the highest TIE laser exposure. Average acuities ranged from a low of 8.5 cpd (3.5 arcmin) to a high of 14.9 cpd (2.01 arcmin). During the same period, the unexposed, left eye acuities were within pre-exposure limits, indicating that, once resumed, task performance was essentially normal.

Video records of the injured right eye were made during brief intervals when the subject viewed the stimulus field with the uninjured left eye. A downward stream of blood from the lesion site was prominent in the video image, and as the eye moved, blood often momentarily swirled upward from the inferior portion of the fundus and then subsided, leaving the vitreous comparatively clear.

Figure 2 shows fundus photographs, taken one

to one-and-a-half hours following laser exposure. All subjects exhibited a white disciform area of altered fundus appearance. Two distinct concentric areas of obscuration were present in Subjects 2 and 3. The innermost area was complexly structured and completely obscured the underlying fundus from view; in the fluorescein angiogram, it was hyperfluorescent. The outer area was translucent white and blood vessels could just be seen through it. Size measurements for both areas were made.

Table 2 lists the initial apparent lesion sizes based on ophthalmoscopic appearance. Since most of the lesions were more nearly elliptical than circular, the radius from the foveolar center to the nearest region of normal appearing fundus was used to measure lesion size. Lesion sizes in horizontal disc diameter (DD) units ranged from 0.59 DD (Subject 1) to 2.00 DD for the largest area of retinal whitening (Subject 3). The centroid of the immense lesion sustained by Subject 3 was slightly offset from the foveola, thus reducing the potential impact of the lesion on acuity. Based on measurement of the minimum radius from the foveola, the equivalent lesion size was 1.41 DD.

Recovery

Grating acuity in both the left and the right eye was tracked from the day of laser exposure (Day 0) until right eye acuity had stabilized by the latter third of the 36-day assessment period. Figures 3 and 4 show daily average acuities for the left and right eyes of the three subjects. With few exceptions, grating acuity in the unexposed left eye of the subjects stayed within pre-exposure baseline limits. Grating acuity in the laser-exposed right eye of the subjects remained below the lower 95% C.I. for five to 14 days (Table 2). Right eye grating acuity eventually recovered to within baseline limits for all subjects, but it rarely exceeded the pre-exposure mean. During the same period, daily average grating acuities for the left, undamaged, eye varied above and below the mean.

The area of apparent retinal damage stabilized in size and developed an irregularly shaped, complexly structured, and mottled appearance. It ranged in size from 0.34 DD to 0.44-0.62 DD, based on fundus photographs taken on post-exposure Day 42. In the fluorescein angiograms, the damaged area was hyperfluorescent; this area contained a small central region, lacking any discernable fluorescence, corresponding to the locus of the initial hemorrhage.

Recovery during the initial post-laser exposure days was associated with distinct vitreous clouding in Subject 2. Figure 5 shows fundus photographs taken at two, seven, 16 and 44 days post-exposure. These should be compared with the clear view of the fundus possible on Day 0 (Fig. 2). Clouding reached a maximum on Day 7. A slight clearing was evident by Day 16, but complete clearing was not documented until Day 44. Coincidentally, return of the subject's right-eye acuity occurred close in time (Day 14) with the beginning of vitreous clearance.

Subject 3 also exhibited vitreous clouding, but it subsided quickly. A different post-exposure complication, striations radiating from the lesion site, developed by Day 16. The striations were still present at Day 36, but had decreased in radial extent compared to Day 16.

Discussion

One of the most interesting effects of laser exposure was the period of time, starting immediately after laser exposure, during which the subjects either did not push the response lever (Subjects 2 and 3), or did so only sporadically (Subject 1). An interpretation of the period of non-responsiveness is that the subjects were effectively blind to any of the grating stimuli. Instances of transient visual 'blackout' have also been reported in laser accident cases[1,22], and might reflect the same phenomenon occurring with the rhesus subjects. An alternative explanation is that the lack of responsiveness was simply a motivational problem induced by the laser exposure. Two observations militate against this explanation. Firstly, each subject did spontaneously resume responding, even in the presence of a large central retinal lesion. Secondly, responding at normal acuity levels occurred immediately when the stimulus channel was switched to the uninjured left eye. The lapse in responding, therefore, would seem to represent a genuine and profound deficit in spatial resolution.

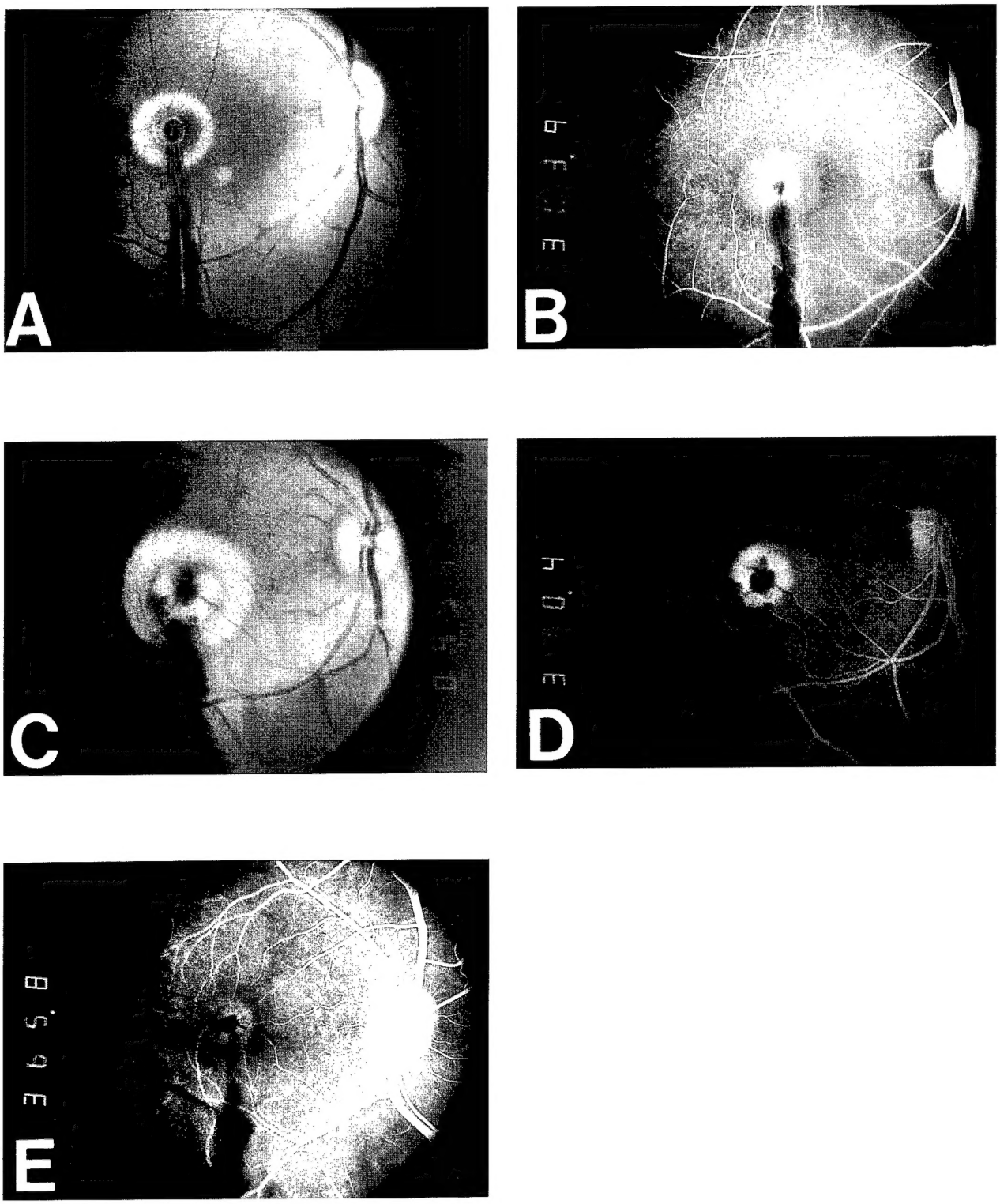

Fig. 2. Fundus photographs taken one-and-a-half hours post-exposure: *a.* white light, Subject 2 (Rh609Z); *b.* fluorescein angiogram, 303.9-sec post-dye injection, Subject 2 (Rh609Z); *c.* white light, Subject 3 (Rh454D); *d.* fluorescein angiogram, 310.4-sec post-dye injection, Subject 3 (Rh454D); *e.* fluorescein angiogram, 365.8-sec post-dye injection, Subject 1 (Rh452D). White light photographs were not available for Subject 1.

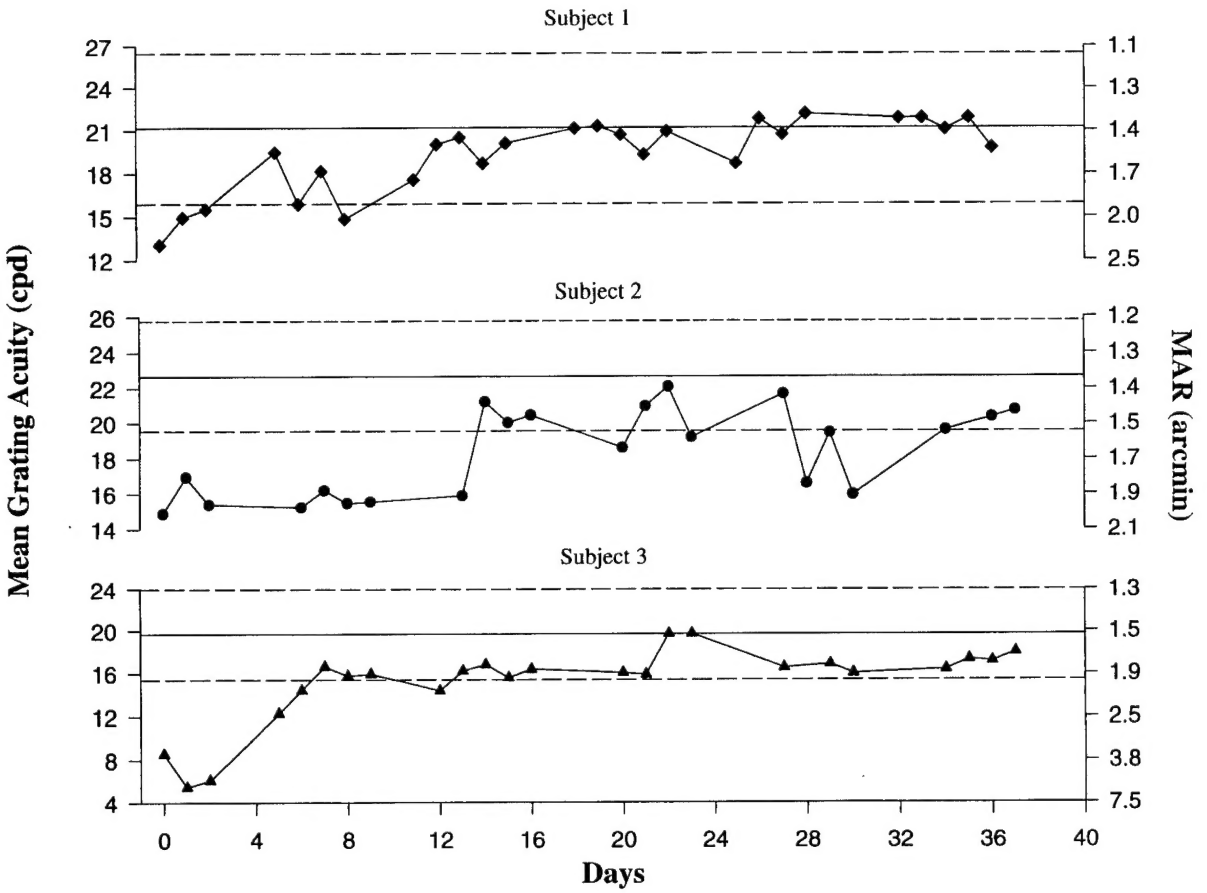

Fig. 3. Post-exposure grating acuity for the laser-exposed right eyes of Subjects 1, 2 and 3. Average acuities for post-exposure sessions are represented by solid symbols; average pre-exposure acuity by the solid horizontal line. The dashed lines symmetrically placed above and below the pre-exposure acuity line are the average upper and lower 95% confidence limits, respectively.

Table 2. Summary of hemorrhage-producing laser exposure and its effect on grating acuity

Measurement	*Subject Number*		
	1	*2*	*3*
Laser total intraocular energy (TIE) (mJ)	0.5	2.5	7.2
Pre-exposure mean acuity (MAR)	1.4	1.3	1.5
Exposure day mean acuity (MAR)	2.3	2.0	3.5
Exposure day acuity range (MAR)	3.9-2.0	3.2-1.2	75-2.6
Final mean acuity (Day 37) (MAR)	1.5	1.4	1.7
Lesion size (DD) – exposure day	0.59	0.56-1.11	1.41
Lesion size (DD) – Day 42	0.38	0.44-0.62	0.34
Initial return to lower 95% CI (days)	5	14	7
Time to first response (min)	1.0	4.6	0.8
Time to first acuity measurement (min)	1.6	6.8	1.1
Time to last acuity measurement (min)	3.0	10.9	24.6
Number of acuity measures	14	40	138

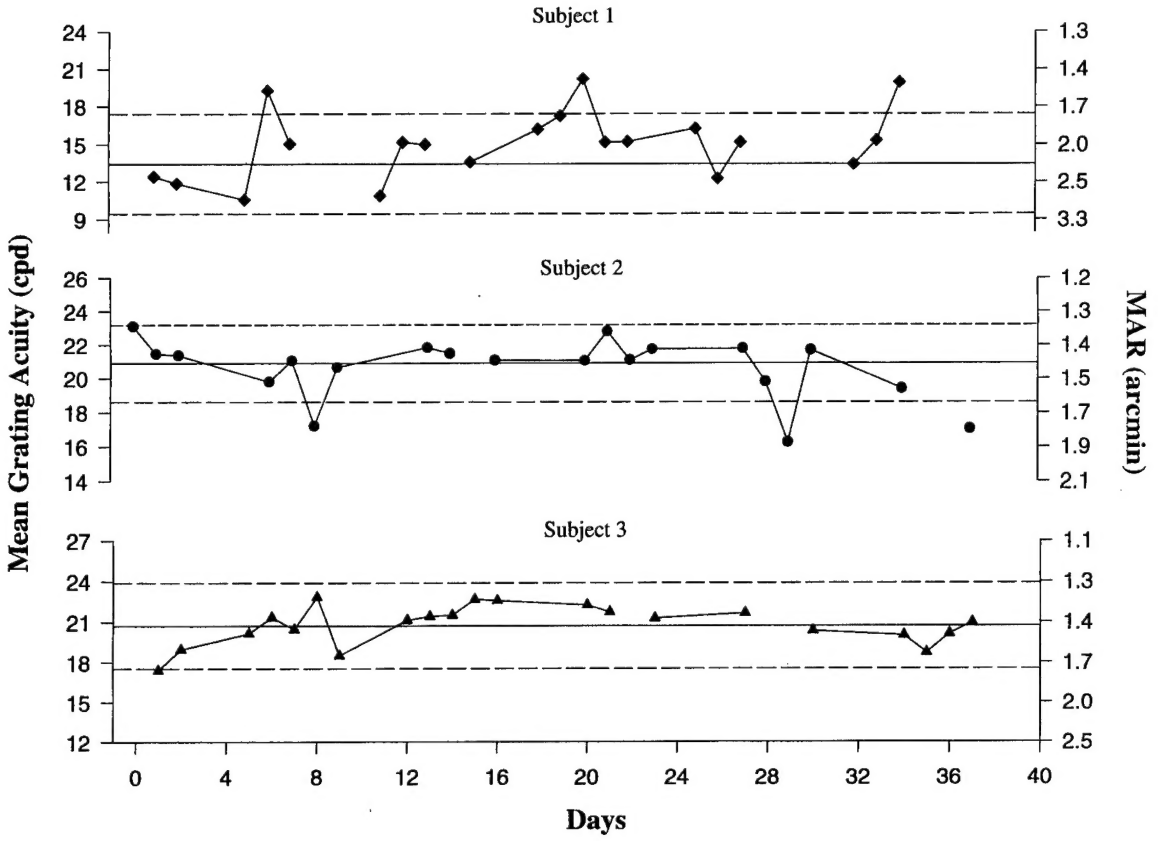

Fig. 4. Grating acuity for the uninjured left eye of Subjects 1, 2 and 3 during the same time interval as shown in *Fig. 3.* The conventions are also the same as those used in *Fig. 3.*

Upon resumption of responding, the average acuity deficit occurring within the first hour following laser exposure was roughly proportional to the area of the funduscopically visible lesion. Some of the transient drops in acuity from the average level might have resulted from translucent veils of blood that varied in position and optical density over time. In the case of Subject 1, an apparently more stationary haze of blood in the vitreous surrounded the frank lesion and could have thereby amplified the area of diminished retinal function. Without an independent measurement of scotoma size, such as perimetry, a more definitive estimate of the affected retina was not possible.

The minimum TIE laser exposure was targeted at 1.10 to 1.5 mJ, a range of values which equals or exceeds the retinal hemorrhage ED90 for a single-pulse, Q-switched foveal laser exposure at 1064 nm in the rhesus monkey[23]. In practice, the TIE proved difficult to control, perhaps because the high peak power of the Q-switched pulse was near the tolerance limits of the optics. The variation of TIE values might have been caused by variable breakdown of the coating on one or more of the mirrors in the optical train. Additional stress was introduced by the need to bring the laser beam to a near focus at several points in the FIMI optics.

With Subject 2, the center of hemorrhage emanation was displaced from the retinal target site, possibly indicating a slight error in targeting. However, an additional hemorrhage site was superimposed on the target area. Perhaps the site of the major hemorrhagic eruption was displaced from the site of laser impingement, but no reports of a similar phenomenon were found in the experimental literature.

The rhesus grating acuity data indicate an overall milder acuity deficit than that in many cases of human foveal, hemorrhagic lesions reported in the laser accident literature. For example, Wolfe[1] pre-

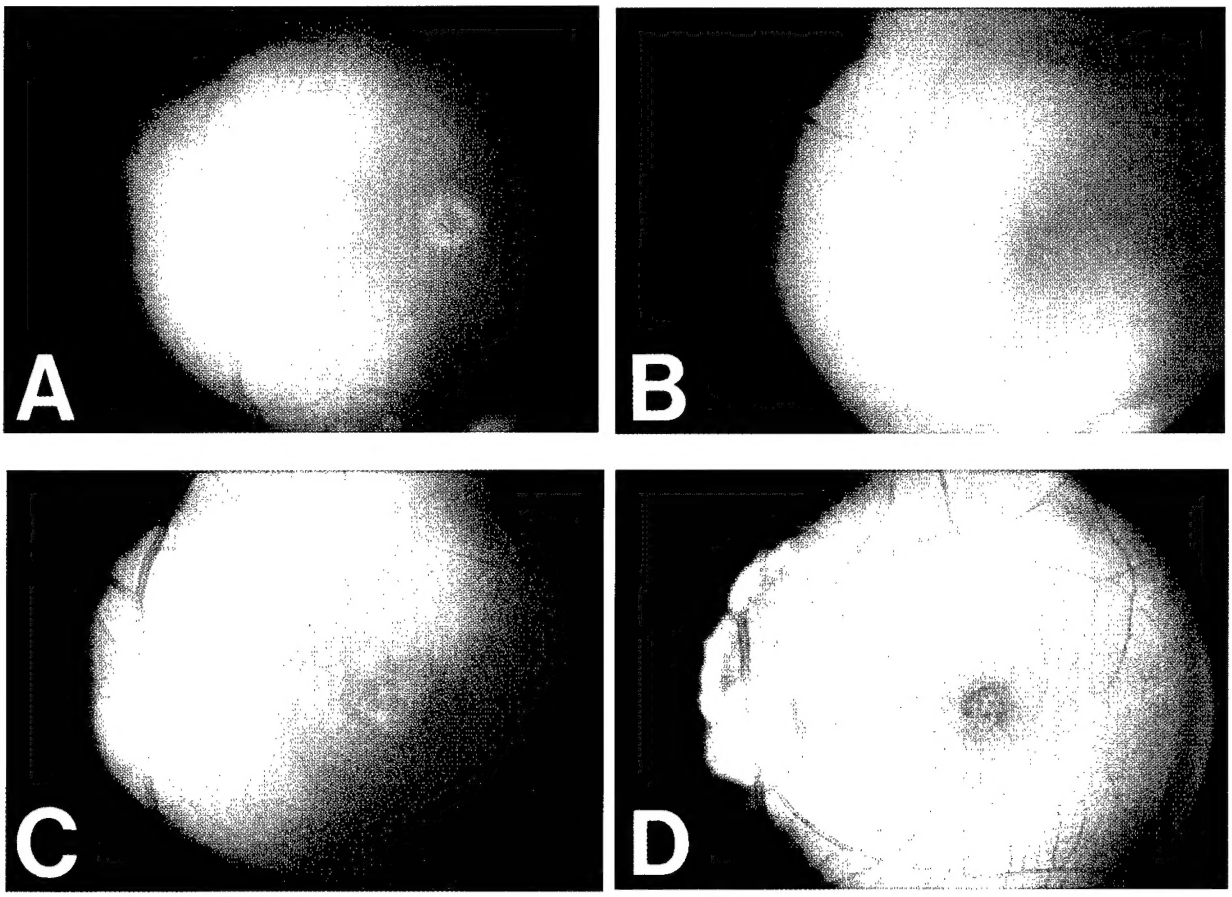

Fig. 5. Fundus photographs, A through D, of Subject 2 (Rh609Z), taken two, seven, 16, and 44 days post-exposure, respectively.

sented six distinct instances of vitreous hemorrhagic lesions in the fovea. Initially measured acuities fell at or above a MAR of 5 arcmin, and recovery acuity levels ranged between 2.50 and 10 arcmin. These findings are comparable with other reports of vitreous hemorrhages[3,24]. Our study showed initial average acuities of 2.00 to 3.55 arcmin, although individual, as opposed to averaged, acuities could be as high as 75 arcmin (0.4 cpd). Subjects recovered to an average acuity of 1.4–1.7 arcmin. These results were reasonably close to those of Glickman *et al.*[2], who also used grating stimuli and rhesus subjects, but overall were less severe than the accident findings. What factors can account for these differences? There is presently insufficient information to attempt a full accounting, but one factor that might have some bearing on this issue is the use of grating stimuli versus the use of punctate acuity stimuli, such as Snellen optotypes or Landolt rings.

Acuity was probably evaluated by Snellen letters in most of the accident cases. The reading of Snellen letters or other standard optotypes might be a more demanding task than grating detection. For instance, the acuity for individual Snellen letters was lower than that for gratings or Landolt rings in a patient with a six-degree central scotoma[25]. Other studies indicate that peripheral acuity, as measured by Snellen letters, is poorer than peripheral acuity measured with gratings[26,27]. Additionally, the reading of contiguous Snellen letters from an eye chart can be a more difficult task than identification of isolated letters[28]. These difficulties could be more pronounced in individuals with newly acquired central scotomas, who have not yet learned effectively to use eccentric fixation.

In comparison to Snellen or Landolt stimuli,

visual acuity measured by gratings could represent a more favorable condition for spatial resolution in the presence of a central scotoma. A grating carries redundant visual information in the form of repeated light and dark bars, and in a testing format such as the one described here, the grating can cover an area larger than the retinal lesion. The observer with a central scotoma might, therefore, find that the detection of a large grating patch is an easier oculomotor task than trying to acquire and resolve the relevant spatial detail in a Snellen letter. One consequence is that the apparent acuity deficit might be less severe than with a small, punctate target. Perhaps the inclusion of large grating patches in the visual function testing battery could expand the clinical perspective on spatial resolution loss in laser-produced retinal injury.

Acknowledgements

The authors would like to thank Dr. Phelps Crump and Capt. Erik Nielsen, Radiation Analysis Branch (AL/OEDA, Brooks AFB), for statistical analyses of the data. Capt. David Beneditz, Laser Branch (AL/OEDL, Brooks AFB), and Mr. David Freeman, KRUG Life Sciences Inc., made significant contributions to the experimental control software. Col. Robert P. Green, Jr., Ophthalmology Branch (AL/AOCO, Brooks AFB), Lt. Col. Leon N. McLin, Jr., Laser Branch (AL/OEDL, Brooks AFB), and Dr. Randolph Glickman (Department of Ophthalmology, University of Texas Health Sciences Center, San Antonio, TX) provided insightful reviews of the manuscript. The Department of biosciences and Bioengineering, Southwest Research Institute, generously supported the revision of this manuscript.

References

1. Wolfe JA: Laser retinal injury. Military Med 150:177-185, 1985
2. Glickman RD, Cartledge RM, Zuclich JA: Visual acuity following laser-induced hemorrhagic lesions in the fovea and parafovea: an experimental study. Proceedings of the 1992 International Laser Safety Conference, Cincinnati, OH, December 1-4, 1992
3. Manning JR, Davidorf FH, Keates RH, Strange AE: Neodymium:YAG laser lesions in the human retina: accidental/experimental. Contemp Ophthalmol Forum 4:86-91, 1986
4. Lang GK, Lang G, Naumann GOH: Accidental bilateral asymmetric maculopathy caused by a ruby laser. (English translation) Klin Mbl Augenheilk 186:331-304, 1985
5. Graham ES, Farrer DN, Mark RG, Fields T: Behavioral assessment of visual function immediately after exposure of the eye to a laser. 6571st Aeromedical Research Laboratory, Technical Report No. ARL-TR-70-9. Holloman Air Force Base, New Mexico, 1970
6. Schmeisser ET: Acute laser lesion effects on acuity sweep VEPs. Invest Ophthalmol Vis Sci 33(13):3546-3554, 1992
7. Harwerth RS, Smith EL III: Rhesus monkey as a model for normal vision of humans. Am J Optom Physiol Opt 62(9):633-641, 1985
8. Merigan WH, Katz LM: Spatial resolution across the macaque retina. Vis Res 30:985-991, 1990
9. Farrer DN, Graham ES, Ham WT Jr, Geeraets WJ, Williams RC, Mueller HA, Cleary SF, Clarke AM: The effect of threshold macular lesions and sub-threshold macular exposures on visual acuity in the rhesus monkey. Am Indus Hyg Assoc J 31:198-205, 1970
10. Weizkrantz L, Cowey A: Comparison of the effects of striate cortex and retinal lesions on visual acuity in monkeys. Science 155:104-106, 1967
11. Yarczower M, Wolbarsht ML, Galloway WD, Fligsten KE, Malcolm R: Visual acuity in a stumptail macaque. Science 152:1392-1393, 1966
12. Zwick H, Bloom KR: Permanent visual change associated with punctate foveal lesions. Invest Ophthalmol Vis Sci (Suppl) 25(3):253, 1984
13. Merigan WH, Pasternak T, Zehl D: Spatial and temporal vision of macaques after central retinal lesions. Invest Ophthalmol Vis Sci 21:17-26, 1981
14. Sperling HG, Wright AA, Mills SL: Color vision following intense green light exposure: data and a model. Vis Res 31(10):1797-1812, 1991
15. Robbins DO, Zwick H: Long wavelength foveal insensitivity in rhesus. Vision Res 20:1027-1031, 1980
16. Crane HD, Steele CM: Generation-V dual-Purkinje-image eyetracker. Appl Opt 24(4):527-537, 1985
17. Crane HD: Stabilized laser coagulator. Technical Report, SRI International, 1979
18. American National Standards Institute: American national standard for the safe use of lasers. Standard Z136.1-1986. New York: American National Standards Institute Inc 1986
19. Cornsweet TN: The staircase-method in psychophysics. Am J Psychol 75:485-491, 1962
20. Levitt H: Transformed up-down methods in psychoacoustics. J Acoust Soc Am 49:467-476, 1970
21. Polyak S: The Retina. New York: University of Chicago Press 1941
22. Thach AB, Lopez PF, Snady-McCoy LC, Colub BM, Frambach DA: Accidental Nd:YAG laser injuries to the macula. Am J Ophthalmol 119(6):767-773, 1995
23. Zuclich JA, Elliott WR, Coffey DR: Suprathreshold retinal lesions induced by laser radiation. Lasers Light Ophthalmol 5(2):51-59, 1992
24. Gabel V-P, Birngruber R, Lorenz B: Clinical observations of six cases of laser injury to the eye. Health Phys 65(5):705-710, 1989
25. Hesse RF, Jacobs RJ, Vingrys A: Central versus peripheral

vision: evaluation of the residual function resulting from a uniocular macular scotoma. Am J Optom Physiol Opt 55:610-614, 1978

26. White JM, Loshin DS: Grating acuity overestimates Snellen acuity in patients with age-related maculopathy. Optom Vis Sci 66:751-755, 1989
27. Herse PR, Bedell HE: Contrast sensitivity for letter and grating targets under various stimulus conditions. Optom Vis Sci 66:774-781, 1989
28. Randall HG, Brown DJ, Sloan LL: Peripheral visual acuity. Arch Ophthalmol 75:500-504, 1966